Performance Analysis of Optical Intra-WBAN Links 1 st

Oussama Haddad, Mohammad Ali Khalighi, Stanislav Zvanovec, Mouloud Adel

Performance Analysis of Optical Intra-WBAN Links

1st Oussama Haddad, 2nd M. Ali Khalighi
Aix-Marseille University, CNRS,
Centrale Marseille, Institut Fresnel
Marseille, France
Oussama.Haddad@fresnel.fr
Ali.Khalighi@fresnel.fr

3rd Stanislav Zvanovec
Department of Electromagnetic Field
Faculty of Electrical Engineering
Czech Technical University in Prague
Prague, Czech Republic
xzvanove@fel.cvut.cz

4th Mouloud Adel
Aix-Marseille University, CNRS,
Centrale Marseille, Institut Fresnel
Marseille, France
Mouloud.Adel@fresnel.fr

***Abstract*—We evaluate the performance of wireless body area networks (WBANs) in medical applications based on optical wireless transmission. We focus on the intra-WBAN links, where a set of medical sensors transmit the measured data to a coordinator node, placed on the patient's body. Based on a Monte Carlo ray-tracing approach and considering the effects of body shadowing and mobility, we propose statistical models for the channel DC gain based on kernel density estimation. Then, we investigate the outage probability performance of the different intra-WBAN links and discuss the impact of user mobility and node placement on the patient's body.**

***Index Terms*—Wireless body-area networks; Optical wireless communications; Link performance; Outage probability.**

I. Introduction

Wireless body area networks (WBANs) are short-range networks, designed to connect wearables in the vicinity of the human body. The use of WBANs has been motivated by technological advances made in many fields of engineering, such as sensor miniaturization, and the development of low power wireless communication technologies. A WBAN consists of a set of sensor nodes (SN), sending their collected data to a coordinator node (CN), placed often on the users body. The CN then forwards these data to an access point (AP) [1]. Typical applications of these networks include medical environments where they can be used for vital signs monitoring and therapeutic stimulations to improve the quality of life of patients and reduce the treatment costs [2].

Current WBAN solutions use generally unlicensed frequency bands in the radio-frequency (RF) domain. However, due to the considerations of electromagnetic interference, data security, and concerns on the impact of RF waves on the human tissues, optical wireless communications have recently received increasing interest, as they can offer an alternative/complementary solution within this context [3], [4].

An important point in studying the performance of optical-based WBANs is to accurately model the user mobility. In fact, the changes in the geometry between the SN and the CN, may cause occasional beam shadowing. A few studies have considered this such as [5], which studied optical intra-WBAN links, i.e., between SNs and the CN, based on Monte Carlo ray-tracing (MCRT) simulations. User mobility was considered based on uniformly distributed random user positions and orientations of the sources/detectors, while the patients body was modeled by a simple rectangular surface. Other works such as [6]–[9] studied the case of extra-WBAN links, i.e., between the CN and an AP.

This paper aims to study the performances of the intra-WBAN links. In contrast to the previous works, we take into consideration both local and global movements of the body, where we model the body parts movement by using a 3D animation of a walk cycle and random trajectories based on a modified random waypoint (RWP) mobility model. We consider two different placements at the shoulder and the hip. Based on channel models obtained through MCRT simulations, we provide statistical channel models using the kernel density estimation (KDE) method. We then evaluate the link performance for a simple on-off keying (OOK) modulation scheme based on the outage probability criterion, given the random time-varying nature of the channel.

The remainder of the paper is organized as follows. In Section II, we present the main assumptions, the considered scenario, and the simulation methodology. Next, we describe in Section III statistical channel modeling and the performance analysis approach. Numerical results including the outage probability for different ambient lighting conditions are presented in Section IV. Finally, Section V concludes the paper.

II. Assumptions and Simulation Methodology

Let us consider the scenario of a patient wearing an intra-WBAN and walking inside a hospital room. We consider the network to have 10 SNs connected to the CN in a star network topology. As it was defined in Section I, both SNs and CN are supposed to be placed on the body. To study the effects of body parts on the link performance, we model the patients body by a detailed 3D mesh that gives an accurate representation of the body parts. We distribute the SNs and CNs over the body as it is shown in Fig. 1. The considered SN positions cover the most likely placements for potential medical applications. Also, we study the effect of CN location by placing it on the shoulder or on the hip, as suggested by [5], [6].

We consider a hospital room of dimensions $(5 \times 5 \times 3)\,\mathrm{m}^3$, which is, for the sake of simplicity, considered here as empty and without furniture. The room has plaster walls and a pinewood floor, where their reflectivity values are given in Table I [10]. To model the patient mobility, we use a 3D animation of a walk cycle to model the relative movement of body parts using Blender [11]. In addition, we generate a random trajectory based on a modified RWP model, where a cubic spline interpolation across the waypoints is performed to get smooth rotations on the user trajectory. By combining these two models, we obtain a set of mobility configurations for our performance analysis. We then use the MCRT-based Opticstudio software of Zemax [12] to get the channel impulse response (CIR) $h(t)$ for each mobility configuration.

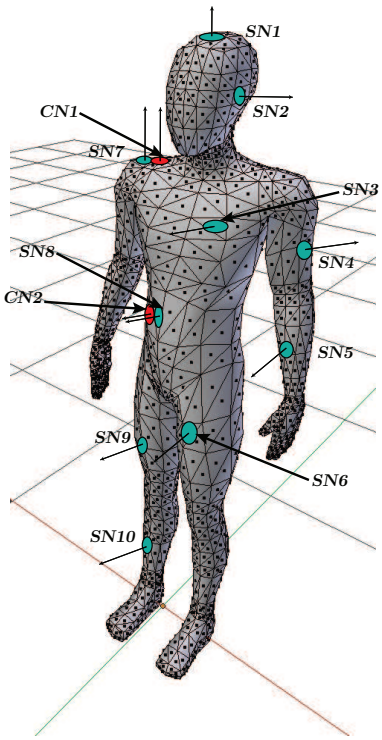

Fig. 1. Considered placements of the CNs and SNs.

To ensure user comfort, we choose to work in the infrared (IR) spectrum. We place at each SN an IR LED of a central wavelength $\lambda_0 = 850\,\text{nm}$ and $\Delta\lambda = 30\,\text{nm}$. The radiation pattern is considered as Lambertian with order $m = 1$, corresponding to a half angle of $60°$ [13]. At the CN, we consider two types of photo-detectors (PD), i.e., PIN and APD, both considered to have an active area of $1\,\text{cm}^2$. Such a large active area is justified by the typical low data rates ($< 1\,\text{Mbps}$) used in medical WBANs [1]. To suppress the visible ambient light, we consider a long-pass absorption filter of $800\,\text{nm}$ cut-on frequency. The receiver (Rx) field-of-view (FOV) is considered as $60°$. Table I summarizes the parameters used in our simulations. Lastly, to quantify the link performance, we will consider the outage probability P_{out}, which is defined as the probability that the bit-error-rate (BER) for a given channel realization is higher than a given threshold BER_{th}.

TABLE I
SIMULATION PARAMETERS.

Tx (SN)	m	1
	λ_0	850 nm
	$\Delta\lambda$	30 nm
Rx (CN) [14]	FOV	60°
	Active Area	$1\,\text{cm}^2$
	$\mathcal{R}$	0.65 A/W
	APD Gain	50
	APD Excess Noise Factor	3
	TIA Load Resistor	$50\,\Omega$
	I_b	$200\,\mu\text{A}$
Room [10]	Dimensions	$(5 \times 5 \times 3)\,\text{m}^3$
	Walls Reflectivity	0.83 (Plaster)
	Floor Reflectivity	0.87 (Pinewood)
	Ceiling Reflectivity	0.83 (Plaster)
Body	Dimensions	$(1.7 \times 0.3 \times 0.2)\,\text{m}^3$
	Reflectivity	0 (absorbing)

III. Performance Analysis

A. Statistical Channel Modeling

We focus here on the channel DC gain H_0, defined as $H_0 = \int h(t)\,dt$. We generate a random trajectory based on the modified RWP and calculate the corresponding H_0 for each point. This results in $N = 516$ realizations of H_0 for each SN and CN link, based on which we propose a statistical model for H_0 based on non-parametric KDE method. This avoids us to do time-consuming MCRT simulations for calculating P_{out}. For a given set of N realizations x_j of a random variable x with a probability density function (PDF) $f_X(x)$, the KDE estimate of the PDF is given by [15]:

$$\hat{f}_X(x) = \frac{1}{N\delta}\sum_{j=1}^{N}\mathcal{K}\left(\frac{x - x_j}{\delta}\right), \tag{1}$$

where $\mathcal{K}$ is the kernel, considered here to be Gaussian, and δ is the smoothing parameter, calculated from $\delta = 1.06\,\hat{\sigma}\,N^{-1/5}$, where $\hat{\sigma}$ is the estimated standard deviation of $\log(x)$ [16].

For instance, we have presented in Figs. 2(a) and 2(b) the histograms of the simulated H_0 together with the fitted PDF based on KDE, for the links between SN3, and CN1 and CN2, respectively. The corresponding δ is 0.06 and 0.11, for the cases of CN1 and CN2, respectively. We notice a good fit between the histograms and the fitted PDF. Meanwhile, we note that the histogram for the case of CN2 is more spread compared to CN1, which is due to shadowing caused by the swing of the right arm during the walk cycle. Also, the mean H_0 is higher for the case of CN2 because the link from SN3 to CN2 experiences first-order reflections, whereas the link to CN1 involves more often second-order reflections.

B. Link Performance Analysis

Using the statistical models obtained in the previous subsection for every SN-CN link, we randomly generated 10^6 values for H_0. Then, for each channel realization, we calculated the BER for an uncoded non-return to zero (NRZ) OOK-based link for given data-rate R_b and transmit power P_t. Assuming optimal maximum likelihood (ML) detection, we have [17]:

$$\text{BER} = \frac{1}{4}\text{erfc}\Big(\frac{\gamma_{\text{th}} - \alpha I_1}{\sqrt{2(\alpha\sigma_{s,1}^2 + \sigma_0^2)}}\Big) + \frac{1}{4}\text{erfc}\Big(\frac{I_1 - \gamma_{\text{th}}}{\sqrt{2(\sigma_{s,1}^2 + \sigma_0^2)}}\Big), \tag{2}$$

where $\text{erfc}(x) = \frac{2}{\sqrt{\pi}}\int_x^\infty \exp(-u^2)du$ is the complementary error function, $\alpha = 0.2$ is the LED extinction ratio, and γ_{th} is the optimal ML threshold that minimizes the BER. Also, $I_1 = \mathcal{R}GP_tH_0$ is the received current for symbol '1', where $\mathcal{R} = 0.65\,\text{A/W}$, stands for the PD responsivity and G is the photo-detector gain ($G = 1$ for PIN and $G = 50$ for APD). Furthermore, $\sigma_0^2 = \sigma_{\text{th}}^2 + \sigma_{\text{b}}^2$, where $\sigma_{\text{b}}^2 = 2eG^2FBI_b$ and $\sigma_{\text{th}}^2 = 4K_bT_eB/R_l$ are the variances of background and thermal noises, respectively [18]. Here, e is the electron charge, K_b is the Boltzman constant, $T_e = 298\,\text{K}$ the equivalent noise temperature, and F is the PD excess noise factor ($F = 1$ for PIN and $F = 3$ for APD), B denotes the Rx low-pass filter, typically approximated by $R_b/2$, and R_L the load resistor of the trans-impedance amplifier (TIA), set to $50\,\Omega$. Also, I_b is

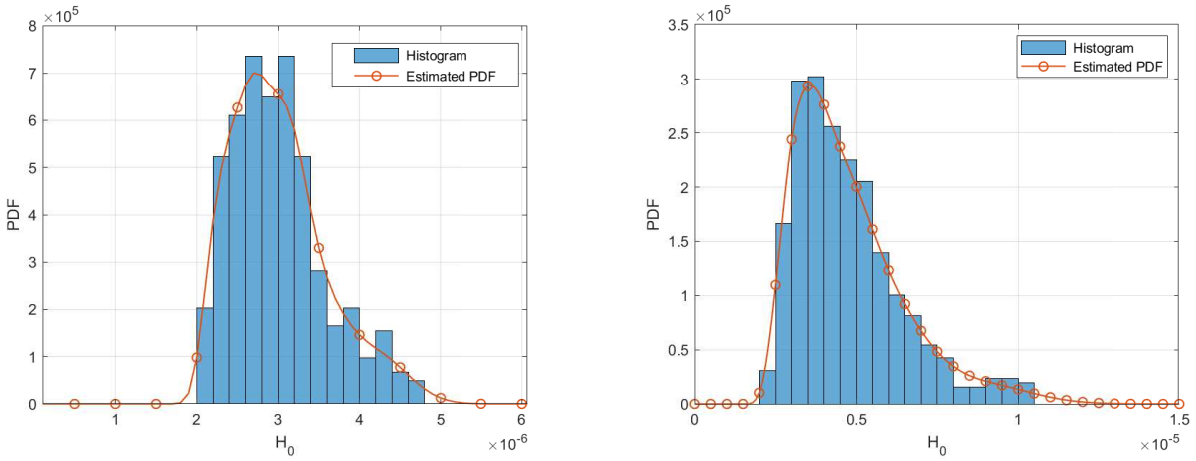

(a) (b)

Fig. 2. Histogram of H_0 for 518 channel realizations of SN3, for the case of (a) CN1 and (b) CN2, and the corresponding estimated PDF by KDE with Gaussian kernel.

the average photo-current generated by a PIN PD due to the background noise [14]. Lastly, $\sigma^2_{s,1} = 2eGFBI_1$ in (2) is the variance of the signal shot noise. We neglect the dark current noise compared with background and thermal noises.

For the case of APD, γ_{th} is calculated as follows [17]:

$$\gamma_{\text{th,APD}} = -\frac{I_1\sigma_0^2}{\sigma^2_{s,1}} + \left(\frac{I_1^2\sigma_0^4}{\sigma^4_{s,1}} + \frac{\alpha I_1^2\sigma^2_{s1} + (1+\alpha)I_1^2\sigma_0^2}{\sigma^2_{s1}} + \frac{(\sigma^2_{s,1}+\sigma_0^2)(\alpha\sigma^2_{s,1}+\sigma_0^2)}{(\alpha-1)\sigma^2_{s,1}} \ln\left(\frac{\alpha\sigma^2_{s,1}+\sigma_0^2}{\sigma^2_{s,1}+\sigma_0^2}\right)\right)^{0.5}. \tag{3}$$

In the case of using a PIN photo-detector, given the negligible signal shot noise [18], we have

$$\gamma_{\text{th,PIN}} = \frac{(\alpha+1)I_1}{2}. \tag{4}$$

IV. Numerical Results

For the considered system, we present here numerical results to study the performance of the intra-WBAN links in terms of outage probability. For P_{out} calculation, we consider $\text{BER}_{\text{th}} = 10^{-3}$. Note that given that P_t is the transmit power for sending an "On" OOK symbol, the average transmit power equals $(1+\alpha)\,P_t\,/2$, with α the extinction ratio.

A. Effect of PD Type and Data-Rate

Let us first compare the effect of link data-rate on the performances of PIN- and APD-based Rxs. For this, concerning the background noise, we set $I_b = 200\mu$A [14]. We have shown in Fig. 3 plots of P_{out} versus P_t for R_b ranging between 1 kbps and 50 Mbps. Here, for the sake of brevity, we show only the link from SN3 to CN1. We reasonably get a lower P_{out} for increased P_{t}, while a higher P_{out} is obtained for increased R_b due to increased thermal noise variance. As expected, APD provides a better performance due to its internal gain: for instance, for $R_b = 200$ kbps and a target P_{out} of 10^{-4}, the required P_{t} is about 41 and 29 mW for the cases of PIN- and APD-based Rxs, respectively.

B. Comparison of Intra-WBAN Links for Low Background Noise Level

Let us now compare the performances of the different links from SNs to CNs. We consider only the case of $R_b = 100$ kbps for both the PIN- and the APD-based Rxs, for the sake of brevity. First, we consider the case of negligible background noise with $I_b = 2\,\mu$A (corresponding to background noise from fluorescent lights [19]), which could correspond to nighttime conditions. We have presented in Fig. 4 plots of P_{out} versus P_t for different SN links and for a PIN-based Rx. Note that the P_{out} values for the APD case are too low for the considered R_b and are not shown here. We notice that, generally, CN1 experiences a better link performance for SNs placed on the upper part of the body. For instance, to achieve a target $P_{\text{out}} = 10^{-4}$, the required P_t for SN7 are 13.5 and 28 mW, for the cases of CN1 and CN2, respectively. Meanwhile, CN2 experiences a better performance for SNs placed on the lower part of the body.

As another important result, we notice that, for the SNs located on the upper part of the body, the P_{out} slopes in the case of CN2 are smaller compared to the case of CN1, which means that CN1 is less affected by intensity fluctuations, or in other words, by channel fading. The inverse holds for the SNs on the lower part of the body, e.g., SN6, SN8 and SN9.

Based on these observations, we can deduce that the choice of CN placement is application dependent. For instance, for EEG applications, most of SNs will be placed on the head, where CN1 is a better choice. On the other hand, for ECG applications, SNs are placed on the heart, arms, and legs, where CN2 position should be preferred. Lastly, note that we can reduce the thermal noise by using a larger R_L, which is feasible given the low data rates needed in our context.

Comparing the results for different SNs, we can deduce the effect of mobility and shadowing. For instance, we notice from P_{out} plots of SN3 and SN5 (placed on the chest and left arm, respectively), that the former link achieves a better performance. We observe the same trend between SN2 and SN4 links. As expected, local mobility results in a degradation of the link performance. Also, from P_{out} plots in Fig. 4(a) of SN3 and

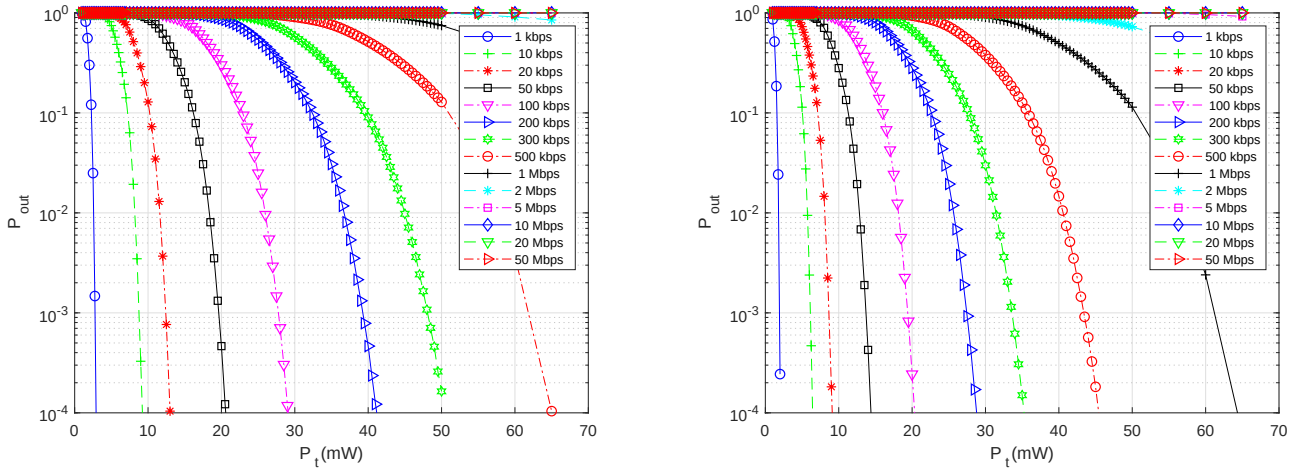

(a) (b)

Fig. 3. P_{out} versus peak transmit power P_t for different data-rates R_b for the case of SN3-to-CN1 link using (a) a PIN (b) an APD. Uncoded NRZ-OOK modulation.

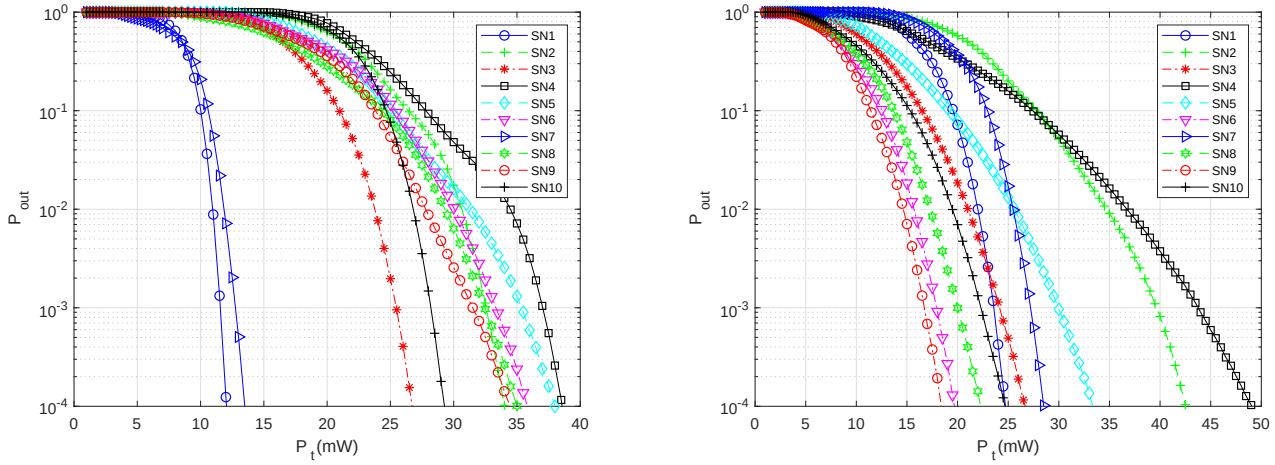

(a) (b)

Fig. 4. P_{out} versus peak transmit power P_t for different SN links and the cases of (a) CN1 and (b) CN2. Low background noise level with $I_b = 2\,\mu$A.

SN10, we notice a better performance for the former for the case of CN1, whereas SN10 achieves a better performance for the case of CN2 from Fig. 4(b). We can explain this by the higher probability of shadowing for CN2, due to the swing of the right arm during the walk.

C. Comparison of Intra-WBAN Links for Relatively High Background Noise Level

Consider now the case of relatively high background noise level with $I_b = 200\,\mu$A, that can be considered as corresponding to daytime conditions [14]. Plots of P_{out} versus P_t for this case are shown in Fig. 5. We notice the same trends between SN-CN links as in the previous subsection with a degradation of the link performances with increase in the background noise level, as expected. For instance, for the case of the PIN-based Rx, the required P_t to achieve the same performances as in the previous case increases for all SNs by approximately 2 to 5 mW. Considering the link form SN5 to CN1, for a target P_{out} of 10^{-4}, the required P_t is 43 mW from Fig. 5(a), while it is 38 mW from Fig. 4(a). Notice that the performance degradation is more significant in the case of the APD-based Rx. This was expected due to the internal gain of the APD.

Comparing PIN- and APD-based Rxs, we observe the same trend between the different SN links, with the APD-based Rx still having a better performance (i.e., requiring a lower P_t to achieve a target P_{out}). For instance, for the link between SN10 and CN2, the required P_t to achieve $P_{\text{out}} = 10^{-4}$ is 54 mW for the case of PIN-based Rx from Fig.5(b), while it is only 37.5 mW when using an APD-based Rx from Fig.5(d).

V. Conclusions

In this work, we studied the performance of optical intra-WBAN links for medical applications. Taking into account the effects of patient's local and global mobility in a room, we proposed accurate statistical channel modeling based on non-parametric KDE. Based on this, we investigated the outage

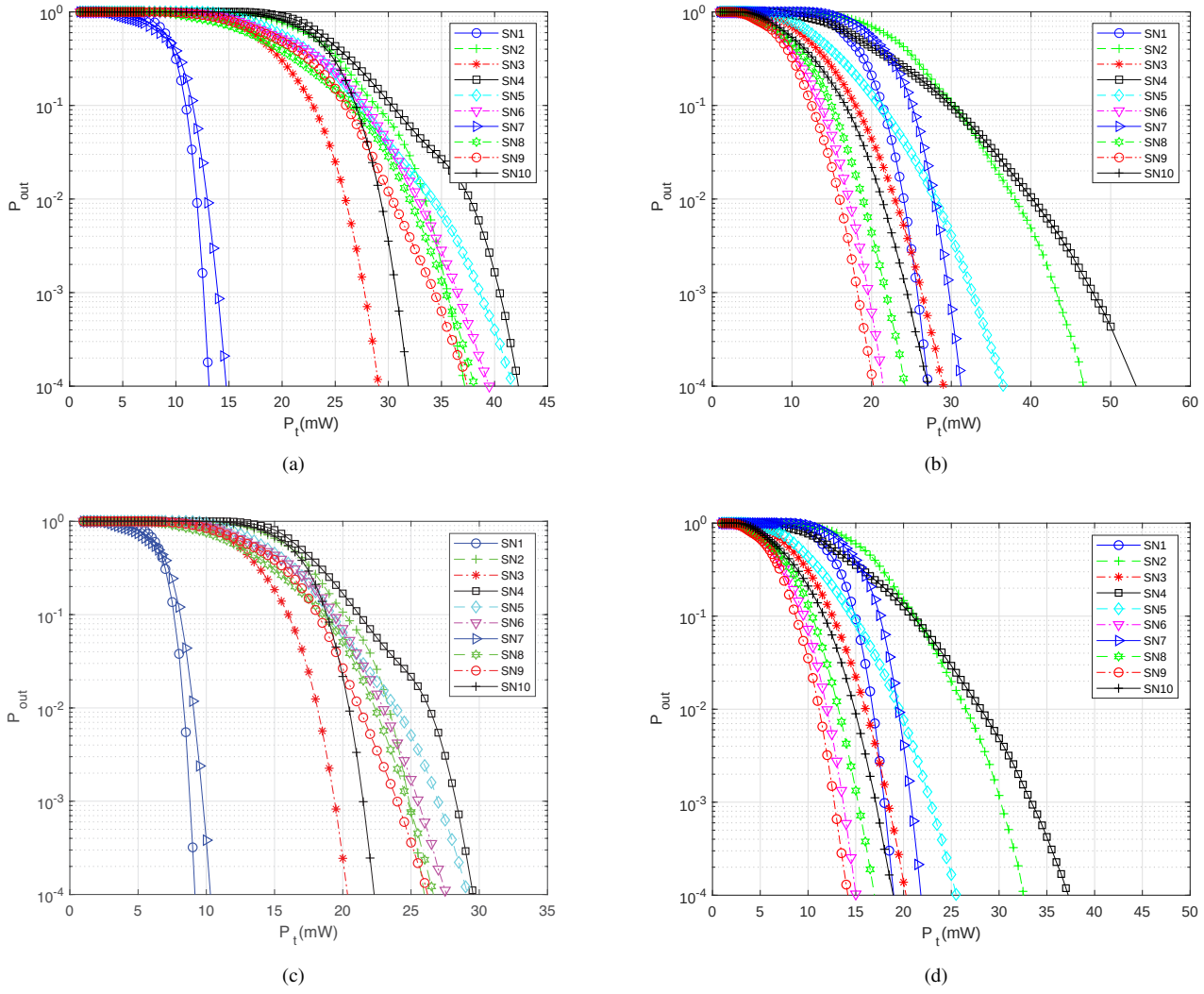

Fig. 5. P_{out} versus the peak transmit power P_t for different SNs for the cases of (a) CN1 with PIN PD, (b) CN2 with PIN PD, (c) CN1 with APD, and (d) CN2 with APD. Relatively high background noise level with $I_b = 200\,\mu$A.

probability performance of different SN-CN links for the two cases of PIN- and APD-based Rxs. We showed the impact on the link reliability of CN positioning, which is related to the effect of link shadowing caused by the body parts movements. We showed that link shadowing resulting from local mobility can cause a significant degradation of the link performance. Therefore, the optimal placement of the CN should depend on the targeted application. We further studied the impact of the background noise depending on the PD type on the required transmit power to ensure a required outrage probability.
Overall, given the generally low levels of required P_t, which remain in the eye-safe region, we can conclude the feasibility of implementing optical WBAN links in practice, in both daytime and nighttime conditions.

Acknowledgment

This work has been supported by VisIoN, a European project funded by the European Union's Horizon 2020 research and innovation program under the Marie Skłodowska-Curie Grant Agreement No. 764461.

References

[1] S. Movassaghi, M. Abolhasan, J. Lipman, D. Smith, and A. Jamalipour, "Wireless body area networks: A survey," *IEEE Communications Surveys & Tutorials*, vol. 16, no. 3, pp. 1658–1686, Jan. 2014.

[2] T. Botsis and G. Hartvigsen, "Current status and future perspectives in telecare for elderly people suffering from chronic diseases," *Journal of Telemedicine and Telecare*, vol. 14, no. 4, pp. 195–203, Jan. 2008.

[3] Z. Ghassemlooy, L. N. Alves, S. Zvànovec, and M. A. Khalighi, Eds., *Visible Light Communications: Theory and Applications*. CRC-Press, 2017.

[4] O. Haddad and M. A. Khalighi, "Enabling communication technologies for medical wireless body-area networks," in *Global LiFi Congress (GLC)*, June 2019, pp. 1–5, Paris, France.

[5] A. Julien-Vergonjanne, S. Sahuguède, and L. Chevalier, *Optical Wireless Communications: An Emerging Technology*. Springer, 2016, ch. Optical Wireless Body Area Networks for Healthcare Applications, pp. 569–587.

[6] T. B. Hoang, S. Sahuguède, and A. Julien-Vergonjanne, "Optical wireless network design for off-body-sensor based monitoring," *Wireless Communications and Mobile Computing*, no. 5473923, pp. 1–13, 2019.

[7] C. Le Bas, S. Sahuguède, and A. Julien-Vergonjanne, "Theoretical and experimental approach for the design of an optical wireless physical activity monitoring system," *International Journal of Wireless Information Networks*, vol. 24, no. 2, pp. 65–77, June 2017.

[8] D. R. Dhatchayeny, S. Arya, and Y. H. Chung, "Patient mobility support for indoor non-directed optical body area networks," *Sensors*, vol. 19, no. 10, 2019.

[9] O. Haddad, M.-A. Khalighi, and S. Zvanovec, "Channel characterization for optical extra-WBAN links considering local and global user mobility," in *Broadband Access Communication Technologies XIV*, vol. 11307, San Francisco, CA.

[10] F. Miramirkhani and M. Uysal, "Channel modeling and characterization for visible light communications," *IEEE Photonics Journal*, vol. 7, no. 6, pp. 1–16, Dec. 2015.

[11] "Blender," https://www.blender.org/, accessed: 29-02-2020.

[12] "Opticstudio," https://www.zemax.com/products/opticstudio, accessed: 29-02-2020.

[13] J. R. Barry, J. M. Kahn, W. J. Krause, E. A. Lee, and D. G. Messerschmitt, "Simulation of multipath impulse response for indoor wireless optical channels," *IEEE Journal on Selected Areas in Communications*, vol. 11, no. 3, pp. 367–379, Apr. 1993.

[14] F. R. Gfeller and U. Bapst, "Wireless in-house data communication via diffuse infrared radiation," *Proceedings of the IEEE*, vol. 67, no. 11, pp. 1474–1486, Nov 1979.

[15] V. Epanechnikov, "Non-parametric estimation of a multivariate probability density," *Theory of Probability and Its Applications*, vol. 14, no. 1, p. 153158, Jan. 1969.

[16] B. Silverman, *Density Estimation for Statistics and Data Analysis*. London: Chapman & Hall/CRC, 1986.

[17] M. T. Dabiri, S. M. S. Sadough, and M. A. Khalighi, "FSO channel estimation for OOK modulation with APD receiver over atmospheric turbulence and pointing errors," *Optics Communications*, vol. 402, pp. 577 – 584, 2017.

[18] F. Xu, M. Khalighi, and S. Bourennane, "Impact of different noise sources on the performance of PIN- and APD-based FSO receivers," in *International Conference on Telecommunications (ConTel)*, June 2011, pp. 211–218, Graz, Austria.

[19] A. J. C. Moreira, R. T. Valadas, and A. M. de Oliveira Duarte, "Characterisation and modelling of artificial light interference in optical wireless communication systems," in *Proceedings of 6th International Symposium on Personal, Indoor and Mobile Radio Communications (PIMRC)*, vol. 1, Sep. 1995, pp. 326–331, Toronto, ON, Canada.